

Dependence of spin susceptibility of a two-dimensional electron system on the valley degree of freedom

Y. P. Shkolnikov, K. Vakili, E. P. De Poortere, and M. Shayegan

Department of Electrical Engineering, Princeton University, Princeton, New Jersey 08544

(Dated: March 22, 2024)

We report measurements of the spin susceptibility, $\chi_{\text{spin}}/g_v g_m$, in an AlAs two-dimensional electron system where, via the application of in-plane stress, we transfer electrons from one conduction-band valley to another (g_v is the valley degeneracy, and m and g are the electron effective mass and g -factor). At a given density, when the two valleys are equally populated ($g_v = 2$), the measured g_m is smaller than when only one valley is occupied ($g_v = 1$). This observation counters the common assumption that a two-valley two-dimensional system is effectively more dilute than a single-valley system because of its smaller Fermi energy.

PACS numbers: 71.70.Fk, 73.43.Qt, 73.50.-h, 71.70.-d

An unsettled question regarding the physics of a dilute, two-dimensional electron system (2DES) concerns the behavior of its spin susceptibility, $\chi_{\text{spin}} = (\mu_B m_0 = 2 \hbar^2) (g_v g_m)$, where μ_B is the Bohr magneton and \hbar the Planck constant, g_v is the valley degeneracy, and m and g are the electron effective mass (in units of free electron mass m_0) and g -factor, respectively. As the 2DES density is lowered, the Coulomb energy of the system dominates over its kinetic energy. A measure of the diluteness is the r_s parameter, the inter-electron spacing measured in units of the effective Bohr radius, or equivalently, the Coulomb energy measured in units of the kinetic (Fermi) energy. Theory [1] predicts that g_m increases with increasing r_s and eventually diverges above a critical r_s , where the 2D electrons attain a ferromagnetic ground state. Experimentally, although there is yet no consensus as to the divergence of g_m , most measurements in dilute 2DESs show an increasing g_m with r_s [2, 3, 4, 5]. In this Letter, we report measurements of g_m in an AlAs 2DES where we change the valley occupation via the application of uniaxial in-plane stress. The data add an interesting twist to this problem as they reveal that, at a fixed density, g_m depends on the valley degree of freedom in an unexpected manner: compared to g_m for a single-valley system, g_m is smaller when two valleys are occupied. This observation appears to be at odds with the widely made assumption that a two-valley system is effectively more dilute than its single-valley counterpart because of its smaller Fermi energy [6, 7, 8].

Our samples contain 2D electrons confined to a modulation doped, 11 nm-wide, AlAs quantum well grown on a GaAs (001) substrate using molecular beam epitaxy [9]. The quantum well is flanked by $\text{Al}_{0.4}\text{Ga}_{0.6}\text{As}$ barrier layers. Using metal electrodes (gates) deposited on the front and back sides of the sample and illumination, we can vary the 2DES density, n , between 2.9×10^{15} and $7.4 \times 10^{15} \text{ m}^{-2}$. In this density range, the low temperature electron mobility is about $20 \text{ m}^2/\text{Vs}$. The resistance is measured using a lock-in amplifier at 0.3K on a Hallbar

sample aligned with the [100] crystal direction. The sample is mounted on a tilting stage so that its orientation with respect to the applied magnetic field can be varied. We studied three samples from two different wafers. Here we present data from one sample; the measurements on other samples corroborate the reported results.

We first show how valley occupancy can be tuned in our samples. In bulk AlAs, conduction band minima (or valleys) occur at the six equivalent X-points of the Brillouin zone. The constant energy surface consists of six half-ellipsoids (three full ellipsoids in the first Brillouin zone), with their major axes along one of the $\langle 100 \rangle$ directions; here we designate these valleys by the direction of their major axes. These valleys are highly anisotropic with longitudinal and transverse effective mass' 1.0 and 0.2, respectively. In an AlAs quantum well with width $\approx 5 \text{ nm}$, grown on a GaAs (001) substrate, biaxial compression due to the lattice mismatch between AlAs and GaAs raises the energy of the [001] valley so that only the [100] and [010] valleys, with their major axes lying in the plane, are occupied [10]. This is the case for our samples. In our experiments, we apply additional, uniaxial compression along the [100] direction to transfer electrons from the [010] valley to the [100] valley while the total 2D electron density remains constant. We measure and compare g_m for the two cases where all the electrons are either in the [100] valley ($g_v = 1$) or are distributed equally between the [100] and [010] valleys ($g_v = 2$). Note that in our work, $g_v = 2$ refers strictly to an equal electron concentration in the two valleys.

We apply stress to the sample by gluing it on the side of a commercial piezoelectric (piezo) stack actuator with the sample's [100] crystal direction aligned to the poling direction of the piezo [11]. Under a positive applied voltage bias, the piezo stack expands along the poling direction and shrinks in the perpendicular directions. This deformation and the resultant stress are transmitted to the sample through the glue. Using this technique, we can achieve a strain range of 4.7×10^{-4} which, for $n < 4.5 \times 10^{15} \text{ m}^{-2}$, is large enough to transfer all the

electrons into a single valley [12]. Since the maximum valley splitting (3 meV) is much smaller than the 150 meV conduction band offset between the AlAs well and the barriers, we expect a negligible strain-induced change ($< 1\%$) in n , consistent with our transport data in perpendicular magnetic fields. Using a calibrated, metal strain gauge glued to the opposite side of the piezo, we monitor the applied strain with a relative accuracy of 5%.

In our experiments, we carefully analyze the frequency composition of the Shubnikov-de Haas oscillations as a function of strain. From such data, we determine the electron densities in the valleys. Additionally, we monitor the dependence of sample's resistance on strain (piezoresistance) at zero and finite magnetic fields. The saturation of the piezoresistance at large (negative) strains signals the onset of the [010] valley depopulation; this depopulation is confirmed by the Shubnikov-de Haas data. From such measurements, we know, for example, that for the data shown in Fig. 1, electrons occupy the [100] and [010] valleys equally in the second trace from bottom (bold), and that for the top two traces (bold) which were taken at strain values of 4.3 and 3.9×10^{-4} , only the [100] valley is occupied (note that these two traces completely overlap in the entire field range).

We employ two commonly used methods to measure g_m . Both involve the application of a magnetic field, B , but each determines g_m at a different degree of spin polarization. In the first technique, we measure the magneto-resistance (MR) of the sample as a function of B applied strictly in the plane of the 2DES (Fig. 1). With increasing B , the Zeeman splitting $E_z = g_B B$ between the electrons with oppositely polarized spins also increases and, at certain field (B_p), equals the Fermi energy, E_F . Beyond B_p , the 2DES becomes fully spin-polarized. At B_p , we have:

$$g_m = (2 \hbar^2 m_0 B) / (n = g_v B_p) : \quad (1)$$

Because of the depopulation of one of the spin subbands at B_p , the electron scattering rate changes, resulting in a kink in the MR trace [2].

We show examples of such traces for $n = 2.85 \times 10^{15} \text{ m}^{-2}$ in Fig. 1. Each trace corresponds to a different amount of strain, between 4.3×10^{-4} and 3.9×10^{-5} , applied along [100]. In all traces, B is also applied along [100]. A pronounced kink is observed in all the traces. The position of the kink is the highest for the top two traces, where all the electrons occupy the [100] valley. As the compression is decreased and the electrons are transferred to the [010] valley, the kink moves to lower fields. The kink's field position is the smallest for the second trace from bottom; for this trace the magnitude of strain is the smallest, and the two [100] and [010] valleys have equal populations. The lowest trace corresponds to positive (tensile) strain along [100]; we again have two unequally populated valleys, but now the [010] valley has

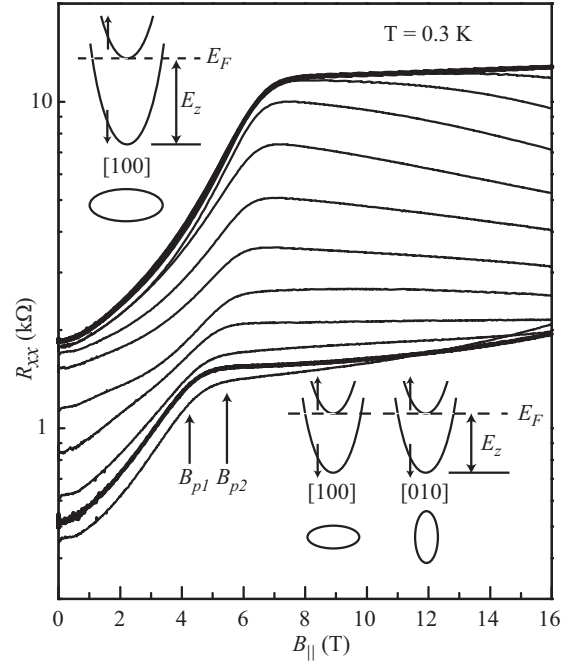


FIG. 1: Resistance of an AlAs 2DES at $n = 2.85 \times 10^{15} \text{ m}^{-2}$ as a function of in-plane field applied along [100]. Strain increases from 4.3×10^{-4} to 3.9×10^{-5} (top to bottom) in steps of 3.9×10^{-5} (thirteen traces are shown, the top two are completely overlapping). Negative strain indicates a uniaxial compression along the [100] direction. In the top two (bold) traces, only the [100] valley is occupied ($g_v = 1$), while the second to the bottom trace (bold) corresponds to the case where the 2D electrons are equally distributed between the two [100] and [010] valleys ($g_v = 2$). The position of the pronounced kink seen in each trace is taken as the field B_p above which the 2DES becomes fully spin polarized. The vertical arrows B_{p1} and B_{p2} mark the possible range $[B_{p1}, B_{p2}]$ of B_p for the lowest trace; we define B_{p1} and B_{p2} as the fields at which the resistance deviates from its exponential dependence on B above and below the kink position. The top and bottom insets schematically show the valley and spin-subband occupations at B_p for $g_v = 1$ and $g_v = 2$, respectively.

a larger population than the [100] valley. For this trace the kink moves back to a slightly higher field.

Associating the kink position with the full spin polarization field B_p , the above behavior can be qualitatively understood from Eq. (1) and the schematic energy diagrams shown in Fig. 1. Given a fixed n , the Fermi energy of the system is twice larger when all the electrons are in one valley ($g_v = 1$) compared to when they are distributed equally between the two valleys ($g_v = 2$). If g_m remained constant, we would thus expect a twice smaller B_p in the case of $g_v = 2$. This simple, non-interacting picture, however, is not quantitatively consistent with the experimental data, which show a reduction of only about 34% in the kink position. According to Eq. (1), this observation implies that g_m for $g_v = 2$ is smaller than for $g_v = 1$.

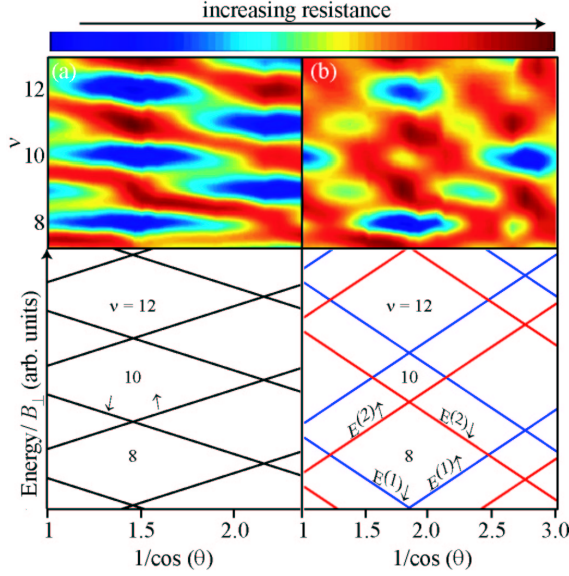


FIG. 2: (color) Angular dependence of the measured magnetoresistance (top panels) and the associated energy fan diagrams (bottom panels) for (a) $g_v = 1$ and (b) $g_v = 2$ AIA S 2DES with $n = 4.32 \times 10^{15} \text{ m}^{-2}$. $E^{(1)}$ and $E^{(2)}$ are the Landau energy levels for the [100] and [010] valleys, respectively.

Before discussing the above observation in detail, we present our measurements of g_m using a second technique, the coincidence method [13], where we no longer restrict B to the plane of the 2DES. With a non-zero B_z (out of plane component of B), Landau levels (LLs), with energy separation equal to the cyclotron energy $E_c = \hbar e B_z / (m m_0)$, form. Each LL is further split by E_z , which is a function of total B . In a typical measurement, we tilt B by an angle from the 2DES normal, such that the in-plane component of B is along the [100] direction, and sweep the magnetic field. At certain θ and B , the energy levels of oppositely spin-polarized electrons coincide at the 2DES Fermi energy. If this "coincidence" occurs when electrons occupy an integer number of LLs (integer filling factor), the MR minimum will rise [13]. At such coincidence, we have $g_m = 2N \cos(\theta)$, where the integer N can be deduced from consecutive coincidences (in θ) at a fixed B . We show an example of such MR data for a case where $n = 4.32 \times 10^{15} \text{ m}^{-2}$ and all the electrons are in the [100] valley ($g_v = 1$) in the top panel of Fig. 2 (a). The corresponding energy level fan diagram is shown in the bottom panel. At all odd $\nu > 7$ (and similarly at all even $\nu > 6$), all of the coincidences are the same. This indicates that g_m is independent of B in this high filling range. From the data shown in Fig. 2 (a), we deduce $g_m = 2.8$.

The data shown in top panel of Fig. 2 (b) were taken for the same n as in the (a) panels, but at zero strain so that the [100] and [010] valleys are equally occupied at $B = 0$. When both valleys are occupied, the dependence

of MR on θ becomes more complicated, with coincidence angles forming a "diamond" pattern with periodicity of four in θ [14]. This dependence of MR can be explained by an energy fan diagram (lower panel of Fig. 2 (b)) in which E_v (energy splitting between valleys) and E_c increase linearly with B_z , and E_z increases linearly with total B and is the same for both valleys [14]. By matching the values of coincidence angles predicted by the energy fan diagram to the experimental data, we extract values for both g_m and E_v . The coincidences at all odd $\nu > 6$ occur at the same θ in data of Fig. 2 (b), implying that g_m is independent of B for high fillings in the $g_v = 2$ case also. From the data of Fig. 2 (b), we find $g_m = 2.2$, again smaller than 2.8 that we find for the case of $g_v = 1$ for the same density.

Figure 3 captures the highlight of our study. It summarizes the results of measurements for the cases where all the electrons occupy the [100] valley or are distributed equally between the [100] and [010] valleys. Plotted are the values of g_m deduced from both the coincidence method, and the kink positions in the parallel MR data and using Eq. (1) [15]. Since the two methods measure g_m at very different degrees of spin polarizations – as low as 20% in the coincidence method, and 100% in the B_p method – the overlap of g_m from these methods asserts that there is negligible non-linearity in spin polarization, implying a nearly constant g_m as a function of spin polarization [16]. To check whether the values of g_m are isotropic, we repeated both coincidence and B_p measurements while applying the in-plane component of the magnetic field along the [010] rather than [100] direction. The data shown in Fig. 3 include results from both field orientations, evincing that g_m is indeed isotropic.

The results presented in Fig. 3 are puzzling. In an independent electron picture, g_m should not depend on the 2D density or the valley degeneracy, clearly in disagreement with the experimental data shown here. Electron-electron interaction, on the other hand, is known to increase g_m as the density is lowered and the system becomes more dilute [1]. This trend is indeed seen in the data of Fig. 3 for both $g_v = 1$ and $g_v = 2$ [17]. At any given density, however, the measured g_m for the $g_v = 1$ case is larger than g_m for $g_v = 2$. This is surprising since the $g_v = 2$ system is expected to be more "dilute" because of its smaller Fermi energy.

In view of our results, it is useful to ask what the proper definition of the r_s parameter for a two-valley system is. This parameter is commonly defined as the ratio of the Coulomb to kinetic (Fermi) energy, $(e^2/4\pi\epsilon_r) = E_F$, where r is the average inter-electron distance. For a one-valley system, r_s is well defined, and is equal to $(l/a_B)(l = n)^{1/2}$, where a_B is the effective Bohr radius. For a two-valley system, there appears to be no clear consensus on the definition of r_s [2, 7, 8]. In all reported definitions, however, it is assumed that, at a fixed density, the two-valley system is equally or more dilute than

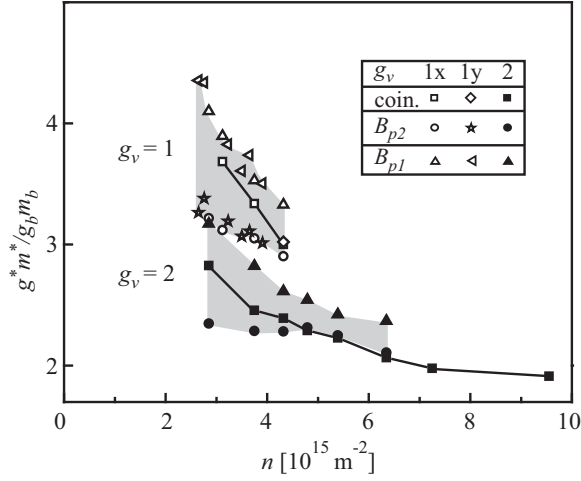


FIG. 3: The product g_m^* in units of $g_b m_b$ (product of band mass and band g -factor) determined from both coincidence and B_p measurements as a function of n . Data are shown for when all electrons occupy the [100] valley ($g_v = 1$, open symbols; orientation of the in-plane component of B along [100] and [010] is indicated by x and y , respectively), or are distributed equally between [100] and [010] valleys ($g_v = 2$, closed symbols). The ranges of possible g_m^* from the parallel field measurements (i.e., $[B_{p1}, B_{p2}]$) are shown as shaded bands. Uncertainty of g_m^* deduced from the coincidence measurement is less than 4%.

the single-valley system. For example, in a model where intervalley interaction is ignored, r_s for the two-valley system is larger by a factor of $\sqrt{2}$ (see for example, Ref. [8]). It is clear from our data, that any definition of r_s that assumes the two-valley system is equally or more dilute than the one-valley system will be in apparent disagreement with our data.

Can our results be explained by some unusual properties of 2DESs in AIs? While we cannot rule out subtle or unknown phenomena, we remark on three possibilities. First, m can depend on valley population if the energy dispersion is non-parabolic. Our measurements [11] of the sample resistance as a function of strain (valley population), while n and B_z (i.e., ϵ) are kept constant, however, provide evidence against this possibility: The resistance oscillates periodically with strain, implying that m does not vary with valley occupancy. Second, it is possible that when $g_v = 2$, the lower Fermi energy of the system leads to its being more susceptible to disorder [18]. While the role of disorder in modifying g_m is not fully known, recent calculations [19] indicate an increase in m when disorder is present; opposite to our observation of a smaller g_m for $g_v = 2$. Third, the Fermi contours in our AIs 2DES are highly anisotropic with a longitudinal to transverse effective mass ratio of approximately 5:1, implying anisotropic Bohr radius for electrons in a given valley. A tantalizing possibility might be that the anomalous behavior we observe is an indica-

tion of anisotropic interaction.

We thank the NSF for support, and E. Tutuc and R. Winkler and K. Karrai for illuminating discussions.

-
- [1] C. Attaccalite et al, Phys. Rev. Lett. 88, 256601 (2002), and references therein.
- [2] T. O kamoto et al, Phys. Rev. Lett. 82, 3875 (1998).
- [3] A. A. Shashkin et al, Phys. Rev. Lett. 87, 086801 (2001).
- [4] V. M. Pudakov et al, Phys. Rev. Lett. 88, 196404 (2002).
- [5] J. Zhu et al, Phys. Rev. Lett. 90, 056805 (2003).
- [6] E. Abraham et al, Rev. Mod. Phys. 73, 251 (2001).
- [7] A. A. Shashkin et al, Phys. Rev. Lett. 91, 046403 (2003).
- [8] M. W. C. Dharma-wardana and F. Perrot, cond-mat/0402253 (2004).
- [9] E. P. De Poortere et al, Appl. Phys. Lett. 80, 1583 (2002).
- [10] K. Maezawa et al, J. Appl. Phys. 71, 296 (1992).
- [11] M. Shayegan et al, Appl. Phys. Lett. 83, 5235 (2003).
- [12] Here we refer to the shear strain, defined as $(L_x = L_x, L_y = L_y)$, where L_x and L_y are the sample dimensions along [100] and [010], respectively. The splitting between the $<100>$ valleys is proportional to this strain.
- [13] F. F. Fang and P. J. Stiles, Phys. Rev. 174, 823 (1968).
- [14] As shown by Y. P. Shkolnikov et al [Phys. Rev. Lett. 89, 226805 (2002)] the valley degeneracy is lifted in the presence of B_z . We find, however, that when strain is zero, valley splitting at all B_z is at its minimum value.
- [15] We use $g_b = 2$ [H. W. van Kesteren et al, Phys. Rev. B 39, 13426 (1989)] and $m_b = 0.46$ [T. S. Lay et al, Appl. Phys. Lett. 62, 3120 (1993)].
- [16] One source for non-linearity of g_m stems from an increase of m when a 2DES with finite layer thickness is placed in a large parallel B . Tutuc et al, Phys. Rev. B 67, 241309 (2003)]. Given the small layer thickness of our 2DES, we expect this increase to be unimportant in our system. This conclusion is further corroborated by our measurements. Mass enhancement due to finite-layer thickness depends on the band mass perpendicular to the orientation of B . Therefore, we would expect a different g_m value when the in-plane field is applied along the major axis of the Fermi contour as opposed to its minor axis; this is contrary to our observation of an isotropic g_m (Fig. 3).
- [17] In a previous study of similar AIs 2DESs but without controlling the valley occupation, E. P. De Poortere et al. [Phys. Rev. B 66, 161308 (2002)] concluded that g_m is nearly independent of density. An assumption was made that, at B_p , all electrons occupy only one valley, regardless of the valley occupation at $B_{jj} = 0$. Data presented here reveal that this assumption was only justified in a narrow range of low densities, for which $g_v = 1$ and valley splitting is significantly larger than E_F .
- [18] As is evident from the data of Fig. 1, the mobility of the 2DES at $B_{jj} = 0$ is smaller when $g_v = 1$. This is not because of larger disorder, but rather a consequence of the geometry of our measurement. Mobility of electrons is determined by the transport mass. When all the electrons are in the [100] valley, transport mass along [100] (the measurement direction) is just the longitudinal effective mass, whose larger value leads to the smaller observed

mobility.

[19] R. Asgari et al., cond-mat/0401289 (2004).